

Article

A Multi-agent Approach to Predict Long-Term Glucose Oscillation in Individuals with Type 1 Diabetes

João Paulo Aragão Pereira ^{1,*}, Anarosa Alves Franco Brandão ^{1,*}, Joyce da Silva Bevilacqua ² and Maria Lucia Cardillo Côrrea-Giannella ³

¹ Computing Engineering Department, Escola Politécnica - Universidade de São Paulo, Brazil; rajoma@usp.br, anarosa.brandao@usp.br

² Applied Mathematics Department, Instituto de Matemática e Estatística - Universidade de São Paulo, Brazil; joyce.bevilacqua@usp.br

³ Laboratory of Carbohydrates and Radioimmunoassays (LIM-18), Hospital das Clínicas (HCFMUSP), Faculdade de Medicina - Universidade de São Paulo, Brazil; maria.giannella@fm.usp.br

* Authors to whom correspondence should be addressed: rajoma@usp.br, anarosa.brandao@usp.br;

Abstract: The glucose-insulin regulatory system and its glucose oscillations is a recurring theme in the literature because of its impact on human lives, mostly the ones affected by diabetes mellitus. Several approaches were proposed, from mathematical to data-based models, with the aim of modeling the glucose oscillation curve. Having such a curve, it is possible to predict, when injecting insulin in type 1 diabetes (T1D) individuals. However, the literature presents prediction horizons no longer than 6 hours, which could be a problem considering their sleeping time. This work presents Tesseractus, a model that adopts a multi-agent approach to combine machine learning and mathematical modeling to predict the glucose oscillation up to 8 hours. Tesseractus uses the pharmacokinetics of insulins and data collected from T1D individuals. Its outcome can support endocrinologists while prescribing daily treatment for T1D individuals, and provide personalized recommendations for such individuals, to keep their glucose concentration in the ideal range. Tesseractus brings pioneering results for prediction horizons of 8 hours for nighttime, in an experiment with seven real T1D individuals. It is our claim that Tesseractus will be a reference for classification of glucose prediction model, supporting the mitigation of short- and long-term complications in the T1D individuals.

Keywords: Glucose Oscillation; Prediction; Multi-agent; Type 1 Diabetes; Personalized; Recommendation

1. Introduction

Diabetes mellitus is a syndrome characterized by hyperglycemia resulting from defects in insulin secretion, associated or not with resistance to the action of this hormone [1]. Diabetes mellitus affects people all around the world, and it is an important health challenge for the 21st century. Type 1 diabetes mellitus (T1D) is the one in which the pancreas produces little or no insulin [1]. This causes glucose concentration control problems, that must be treated with insulin injection and frequently causes long-term complications. Currently, more than 1.1 million children and adolescents under the age of 20 have T1D around the world [2].

There are several challenges faced by researchers and health professionals, mostly related to developing means to provide treatments that bring better results in terms of short-term glucose control and risks reduction of developing long-term complications.

Efforts to address these challenges come from academia to the pharmaceutical industry. From the theoretical and technological point of view, several models were proposed to support the avoidance of hypoglycemic or hyperglycemic conditions in T1D individuals. Moreover, there are models that mimic the dynamic exchange of information between the components of the human glucose-insulin regulatory system (HGIRS) [3]. Nevertheless, at the best of our knowledge, they are still unable to predict the glucose oscillation curve for intervals greater than 4 hours.

This paper presents Tesseract, a hybrid model that adopts a Multi-Agent System (MAS) [4] approach to combine math and data-driven techniques to predict the glucose oscillation up to 8 hours for individuals with T1D. As *tesseract* has 4-dimensions [5], Tesseract has 4 main agents, namely (i) the recommender; (ii) the predictor; (iii) the mathematical, and (iv) the machine learning (ML). In addition, the model also has reactive agents to receive external data from the T1D individual and intelligent agents to monitor and control inputs and outputs along the system execution.

Tesseract predicts the behavior of the glucose oscillation taking into account basal and fast-acting insulin infusion; current glucose concentration; food (carbohydrate, protein and fat) and alcohol intake; and physical activity. Having such information the model is able to present the predicted glycemic curve for a time interval up to 4 hours during the day and up to 8 hours during the night.

This paper is organized as follows: section 2 (HGIRS) presents a brief description of the Human Glucose-Insulin Regulatory System and its associate mathematical model. Section 3 present some related work and section 4 presents Tesseract model itself, its architecture and functioning. After, we present the experimental results on section 5 and finally conclude the paper in section 7.

2. Human Glucose-Insulin Regulatory System

The HGIRS is part of the human endocrine system [6], and is comprised of two main hormones, insulin and glucagon, produced and released, respectively, by β and α -cells of the pancreatic islets. These two hormones, that exert opposing effects, act in concert to maintain blood glucose (BG) in a narrow range. During the fasting state, glucagon stimulates hepatic glucose production (HGP) in order to prevent hypoglycemia while insulin is secreted at levels sufficient to constrain HGP and to maintain BG concentration at approximately 90 mg/dL (basal secretion). After meals, the increase in BG concentration stimulates insulin secretion (meal-related secretion), suppressing HGP and stimulating glucose uptake by insulin-sensitive tissues such as muscle and adipose tissue, eventually restoring normoglycemia.

Insulin secretion is complex and glucose is the most potent stimulant of insulin release. After 8 to 10 min of food ingestion, insulin concentration increases, reaching a peak in 30 to 45 minutes, and then rapidly decreasing to baseline values in 90 to 120 minutes [7]. Insulin is a physiological suppressor of glucagon release, thus, glucagon secretion is low in the postprandial period. On the other hand, glucagon is released during fasting, when BG is in the normal range and insulin concentration is low [7].

In the case of T1D, autoimmune destruction of pancreatic β -cells prevents insulin secretion. Thus, T1D individuals depend on exogenous insulin administration to mimic the physiological secretion of this hormone, i.e., basal and meal bolus insulin. To maintain BG concentration as close as possible to the normal range, it is also necessary to measure BG and to count the amount of macronutrients (especially carbohydrates) before every meal to calculate the bolus insulin dose, that must match the total carbohydrate content of that meal and also correct occasional hyperglycemias.

Optimal glycemic control is crucial to avoid the complications associated with chronic hyperglycemia. However, the procedures described above are relatively complex and are influenced by numerous other factors, such as type and intensity of physical activity, as well as stress, among others, which impair glycemic control, contributing to the occurrence of episodes of hyper and hypoglycemia. The literature presents several predictive models

for glucose oscillation like [8], [9], [10] and [11], being the last one with night prediction of up to 6 hours. However, we could not find any model that predict glucose oscillation, in a continuous and personalized way.

Quantitative methods to model metabolic physiology of T1D individuals are usually based on ordinary differential equations (ODE), and are also called compartment models [12]. We propose an extension to the model proposed by Kissler et al (2014) presented in equation (1), which adopts the glucose compartment: $G'(t)$.

$$G'(t) = G_{in} + f_1(I(t - \tau_2)) - f_2(G(t) + \gamma[1 + s.(m - m_b)].(f_3(G(t)).f_4(I(t))) \quad (1)$$

In that model f_1 describes HGP; f_2 describes the central nervous system glucose utilization; f_3 describes the muscle/fat glucose utilization; f_4 describes the muscle/fat insulin uptake; and f_5 describes the pancreatic insulin production. The parameters semantics are given in table 1.

Table 1. Parameters: compartment models

Symbol	Description
I_{in}	Insulin infusion rate
G_{in}	Glucose intake rate
β	Relative pancreatic β -cell function
γ	Relative insulin sensitivity
s	Rate of insulin sensitivity increase per minute of exercise
m	Daily minutes of physical activity
m_b	Baseline minutes of physical activity
V_{max}	Maximum insulin clearance rate
K_M	Enzyme's half-saturation value

Our extension considers the approach proposed by Schindelboeck et al (2016) for describing f_1 in compartment $G'(t)$, to consider alcohol ingestion and replace γ proportionally by $eGDR$ – the estimated glucose disposal rate ((milligrams per kilogram per minute)), following the approach of Epstein et al (2013). Nevertheless, we completely exchange compartment $I'(t)$ by building polynomial equations from the pharmacokinetics data of four types of insulin. This mathematical modeling is the core of our Mathematical agent and is described in the following.

2.1. A mathematical model for HGIRS

The glucose equation $G'(t)$ (glycemic value as a function of time) should be calculated and is directly related to the amount and type of macronutrients ingested as well as the time (Δt_{ex} – measured in minutes) and intensity (VO_2 – maximum volume of oxygen consumed) of physical exercise [15] and [16], in accordance with [17].

The value of $Gluc_0$ (glycemia in $t = 0$) comes from the glucometers, either continuous and automatic or manual (capillary) measurement. The G_{in} and I_{in} values refer to the rate of glucose intake and insulin infusion, respectively. G_{in} is measured in $mg/dL.min$, varying in the interval $[0, 1.08]$. The insulin equation $I'(t)$ (insulin concentration value as a function of time) and the value of I_0 (insulin concentration at $t(0)$) come from the pharmacokinetics equations of each type of insulin, selected by each individual.

Thus, with two equations modeled, we feed our Mathematical agent with them in order to start the labeling of our dataset, as well as to support the continuous learning in Tesseractus.

2.1.1. The glucose equation 114

The description of how the glucose compartment is modeled by using a similar approach of the one from equation 1, extending f_1 and reusing f_2 , f_3 and f_4 . Also, we rename the physical exercise contribution to the model ($f_{ex} = [1 + s(\Delta t_{ex} - \overline{\Delta t_{ex}})]$). Therefore, it is represented by 115
116
117
118

$$G'(t) = \overbrace{(G_{in} + f_1(I(t - \tau_1)))}^{\text{glucose production}} - \underbrace{(f_2(G(t)) + \gamma f_{ex} \cdot (f_3(G(t)) \cdot f_4(I(t))))}_{\text{glucose consumption}}$$

Our extension in f_1 considers the fact that there are two sources of glucose production: (1) the metabolism of ingested macronutrients, mainly carbohydrates, and glucose intake (G_{in}) is not usually constant; and (2) originated in the liver (HGP) [3]. In this case, glucagon exerts control over the liver and causes it to dispense glucose, with a slight delay (given by τ_1) of between 15 and 20 minutes [18]. In order to allow personalization, we define f_1 considering or not alcohol ingestion, following the understanding of Schinzelboeck et al 2016. Both equations (2) and (3) use the reference values proposed by [19], [20] and [21]. Then, for HGP_{max} is $180mg/min$, α is $0.29L/mU$, V_{pla} is $3L$, and C_5 is $\mu U/L$. Here, HGP_{max} stands for hepatic glucose production, α for hepatic sensitivity to changes in insulin, V_{pla} for the volume of plasma in the body, C_5 for the insulin concentration at which the liver is most efficient, and $A_g(t)$ for alcohol ingestion. 119
120
121
122
123
124
125
126
127
128
129

$$f_1(I(t - \tau_1)) = \frac{HGP_{max} \cdot (1 - A_g(t))}{(1 + \exp(\alpha(\frac{I(t)}{V_{pla}}) - C_5))} \quad (2)$$

or

$$f_1(I(t - \tau_1)) = \frac{HGP_{max}}{(1 + \exp(\alpha(\frac{I(t)}{V_{pla}}) - C_5))} \quad (3)$$

2.1.2. The exogenous insulin equation 130

Our approach adopts the pharmacokinetics data of four types of insulin (glargine [22], degludec [23], lispro [24] and aspart [25]) to support this modeling based on the approximation of polynomial functions. Since industry information is not enough for producing a viable approximation, we combined them with information from a dataset of seven real Brazilian volunteers that use such insulins to derive the polynomial functions related to each of them. The dataset is described in subsection 5. 131
132
133
134
135
136

For instance, for glargine, an insulin of slow action, we got values from [26], [27], [28], [29], and [30], as well as the FDA report [22] and the industry representative information [31]. On the other hand, for lispro, an insulin of fast action, we got values from [32], [33], [34]. The insulin lispro report produced by FDA [35] was used to confirm the time-of-action and pharmacokinetic information. Having such values, we were able to build a polynomial function y that provide an approximation for the exogenous insulin compartment. Each point of y represents the concentration of insulin prescribed at a given time (t), considering the parameters of the T1D individual. 137
138
139
140
141
142
143
144

Figure 1 presents an example of a polynomial curve y for glargine, to cover a 24h period of time. It can be observed that y is a combination of y_1, y_2, y_3, y_4 and y_5 , where y_1 and y_3 have degree 4, y_2 has degree 2, and y_4 and y_5 have degree 3.

$$\begin{aligned}y_1 &= -0.0259x^4 + 0.4255x^3 - 2.5787x^2 + 7.213x + 9.5966 \\y_2 &= 0.105x^2 - 2x + 26.655 \\y_3 &= -0.0996x^4 + 3.8587x^3 - 57.701x^2 + 379.78x - 910.29 \\y_4 &= -0.0808x^3 + 3.5536x^2 - 52.254x + 269.54 \\y_5 &= -0.011x^3 + 0.6492x^2 - 13.24x + 102.98\end{aligned}$$

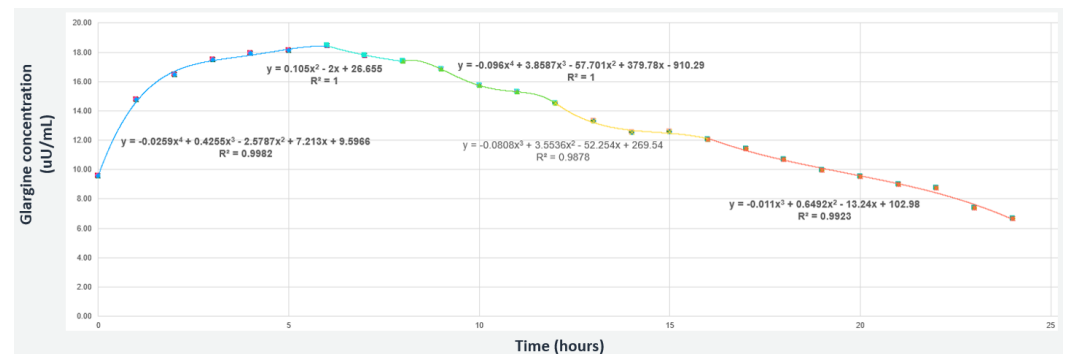


Figure 1. Glargine insulin (slow-acting) - ex: 0.36U/Kg concentration.

Figure 2 presents an example of a polynomial curve y for lispro, to cover a period of time of 300 minutes. It can be observed that y is a combination of y_1, y_2, y_3, y_4, y_5 and y_6 , where y_1 and y_4 have degree 3 and y_2, y_3, y_5 and y_6 have degree 2.

$$\begin{aligned}y_1 &= -0.0015x^3 + 0.0752x^2 + 0.0473x + 0.0829 \\y_2 &= -0.0022x^2 + 0.2445x + 23.638 \\y_3 &= -0.0097x^2 + 0.9403x + 7.5778 \\y_4 &= 0.00002x^3 - 0.0059x^2 + 0.3791x + 23.134 \\y_5 &= 0.0004x^2 - 0.2612x + 42.877 \\y_6 &= 0.000006x^2 - 0.0822x + 22.163\end{aligned}$$

3. Related Work

This section presents some models that provide hybrid solutions for the predictive modeling of glucose oscillation for T1D. Hybrid solutions usually combine mathematical modeling with data-driven techniques. In a literature search, [8],[9],[10],[36], presented hybrid predictive models with PHs from 90 to 120 minutes. Nevertheless, for [37], [38],[39],[40],[41],[16],[42],[43],[44],[45],[46], the prediction horizon (PH) varies from 30 to 60 minutes.

Georga and colleagues 2013 adopted a multivariate regression approach, to derive a predictive model for subcutaneous glucose concentration prediction in T1D individuals. The method was evaluated with a dataset composed of twenty-seven real T1D individuals and presented an average prediction mean square errors of 5.21 mg/dL for 15-min, 6.03 mg/dL for 30-min, 7.14 mg/dL for 60-min, and 7.62 mg/dL for 120-min PHs. Liu and colleagues 2019 presented a glucose forecasting algorithm suited for long-term PHs. The algorithm is based on compartmental models for the HGIRS. It was evaluated with clinical data of ten real T1D individuals. For a 120-min PH, an improvement of 18.8% on prediction accuracy measured with the root mean square error (RMSE), 17.9% A-region of error grid analysis (EGA), and 80.9% hypoglycaemia prediction calculated by the Matthews correlation coefficient. Cescon, Johansson and Renard 2015 presented a subspace-based linear multi-step predictor as a predictive model for short-term glucose oscillation. The model was evaluated with seven real T1D individuals and had obtained the prediction error

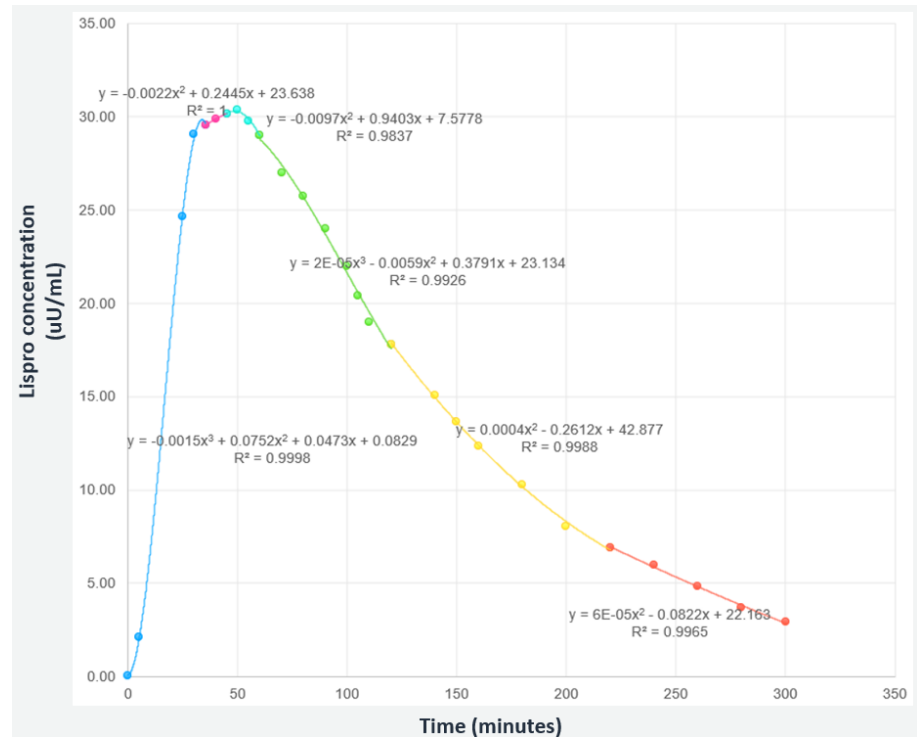


Figure 2. Lispro insulin (fast-acting) - ex: 0.16U/Kg concentration.

standard deviation of 58.06 mg/dL on 120-min. Contreras and colleagues 2018 combine physiological models for HGIRS with grammatical evolution as a search-based technique to design a predictive model for short-term glucose oscillation. Considering the Clarke error grid, they achieved more than 96% results falling inside regions A and B for 90-min.

Since there are T1D individuals that feed at intervals greater than 2 hours, their results are not helpful for them. The proposal of the Tesseract model is to extract the best features of each approach (physiology, data and multi-agent) in order to reach a longer PH, at personalized intervals of 4 hours in the full daytime period, and 8 hours in the night period, keeping the MAE below 28 mg/dL in both periods and for all PHs. A discussion of the results is in the section 5.

4. Tesseract model

Tesseract adopts a multi-agent approach to define a hybrid model to predict the glucose oscillation up to 4 hours during daytime and up to 8 hours at night period. It is a hybrid model because agents are defined using both, compartment models (described in sec 2.1) and data-driven techniques, such as machine learning (ML). Tesseract has two types of agents: reactive agents and intelligent agents. Nevertheless, we decompose the problem in such a way that each agent is responsible for a portion of the phenomenon [47], which means that there are several agents of each type. The reactive agents are responsible for collecting data and feeding intelligent agents with the collected data or for monitoring data, error, and ODE parameters. Intelligent agents are responsible for using data to predict the glucose oscillation. The intelligent agents are: the Recommender agent, the Predictor agent, the ML agent and the Math agent.

The Recommender agent has a knowledge base composed of labeled glucose oscillation prediction curves (within the range or out of range - following a semaphore metaphor) and it is responsible for finding and labeling suitable curves for received data from and delivering them to the user. The Predictor agent has a knowledge base of labeled predicted values and actions and it is responsible for asking for the Math and the ML agent information to populate its knowledge base and for providing glucose oscillation prediction curves for the Recommender agent. The Math agent has the math modeling presented in sec. 2.1

as the core for the generation of glucose oscillation prediction curves, and the ML agent learns the glucose oscillation prediction curves from the combination of received data provided by reactive agents and by the Math agent. Communication is bidirectional between intelligent agents. The Predictor agent communicates with all intelligent agents, and the ML agent communicates with the Predictor and the Math agents. Reactive agents only send messages to intelligent agents. Having received these messages, intelligent agents act accordingly to recommend a glucose oscillation prediction curve or adapting the recommendation given the monitored context (prediction error above a threshold, need for updating the ODE parameters or non conformance of collected data as expected).

Tesseractus innovates in the problem solution by adopting a learning policy that considers both, information from the individuals collected data and from the mathematical modeling. Therefore, at the very beginning we define a set up step, for knowledge acquisition and data labeling. In this step, the Math agent generates glucose values and associated labeling, providing information to accelerate the learning, using the generated glucose values and associated labeling, and the ML agent reuses knowledge from the Math agent. All intelligent agents knowledge bases are built in a continuous reinforcement learning cycle, that begins with the Math agent knowledge combined with a reward policy based on the semaphore metaphor. Data is labeled green, yellow or red depending on the glucose concentration and the absolute error, both within pre-established thresholds. The reader may observe in table 2 that there are two rewards labeled as green and other two rewards as red because excellent and normal glucose levels associated with absolute error smaller than 30 mg/dL are labeled as green, depending on the PH; and hyperglycemia and hypoglycemia levels are labeled as red, as well as absolute error bigger than 30 mg/dL. For the red label the reward should be considered with at least one of the situations occur. Acceptable glucose concentration is labeled as yellow. By absolute error we mean the error between the measured and the predicted glucose values.

Table 2. Tesseractus reward policy.

State	Reward
Green	10
Green	8
Yellow	0
Red	-5
Red	-10

The architecture of Tesseractus is presented in figure 3, where numbers are adopted to support its explanation flow.

1. Reactive agents collect data from continuous glucose monitors (CGM), voice or manually and send them to the Recommender agent;
2. Recommender agent receives data, associate it with its time frame creating a tuple $\langle data, time \rangle$ and checks its knowledge base (KB) if there are actions to be taken related to them;
3. if yes, the predicted oscillation curve is labeled in the ideal range (80-120 mg/dL during fasting, and up to 160 mg/dL in postprandial periods), stored in the KB as $\langle time, label, curve \rangle$, and sent it to the user;
4. if not, the Recommender agent requests information about prediction curves to the Predictor agent;
5. the Predictor agent checks its KB to see if there is a suitable prediction curve. If don't, it propagates the request to the ML and Math agent;
6. the ML agent and Math agent, at a given time frame, store the prediction values in their KB and return the value linked with prediction calculation to the Predictor agent;
7. the Predictor agent analyzes the value received and, if it is a value that is in the ideal range, the Predictor agent sends a return message to the Recommender agent,

adopts an approach similar to active learning. Figure 4 depicts this learning flow that is described next.

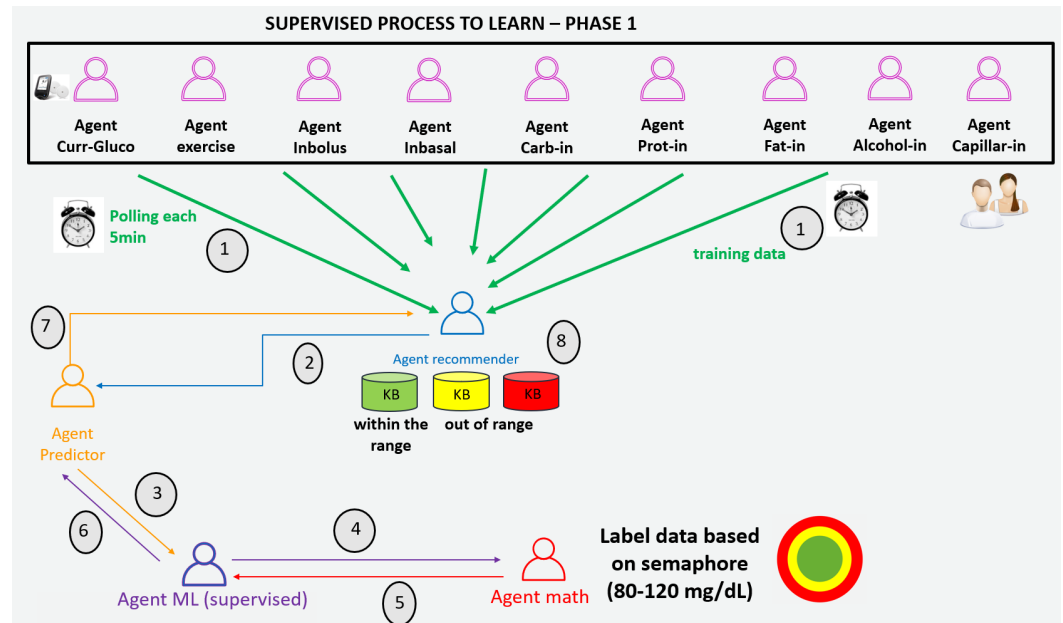


Figure 4. Tesseract set up: acquiring knowledge.

1. reactive agents collect environmental information via sensors (every 5 min from GCM), by voice or manually;
2. the Recommender agent receives data, and asks to the Predictor agent to calculate and generate the glucose curve;
3. the Predictor agent asks the ML agent to create a timestamp and generate the glucose curve;
4. the ML agent asks the Math agent for labeling the generated value, based on the predefined semaphore;
5. the Math agent forward the labeling payload to the ML agent;
6. the ML agent sends to the Predictor agent the timestamp, glucose curve, predictions and label, based on the data received;
7. the Predictor agent receives the message and forwards it to the Recommender agent;
8. the Predictor agent receives the new information and classifies it in each KB according to the received label (green, yellow and red).

4.2. Tesseract functioning

After the set up, Tesseract starts its functioning, in a continuous learning cycle based on Reinforcement Learning with receipt of new data provided by the reactive agents in order to carry out the validation of values.

The Math and ML agents generate knowledge for the Recommender and Predictor agents. In addition, they also take advantage of information provided by the other reactive agents, in order to update and/or correct the values of the parameters used in the ODE that are the core of the Math agent. Moreover, we consider the time series associated with the green labeled data to adopt the sliding window approach [52] and achieve different PHs, from 15 min to 8 hours. In fact, since the glucose concentration dataset is measured each 5 minutes, the ML agent used the last 2 hours of historical data about carbohydrate and 5 hours about bolus insulin to predict it. These time slots were chosen based on the duration of carbohydrate metabolism and the average time of fast-acting insulin action in the human body, respectively. In figure 5, insulin values sliding window (5 hours) is represented by the black dashed left-right arrow, while carbohydrate values sliding window (2 hours) are

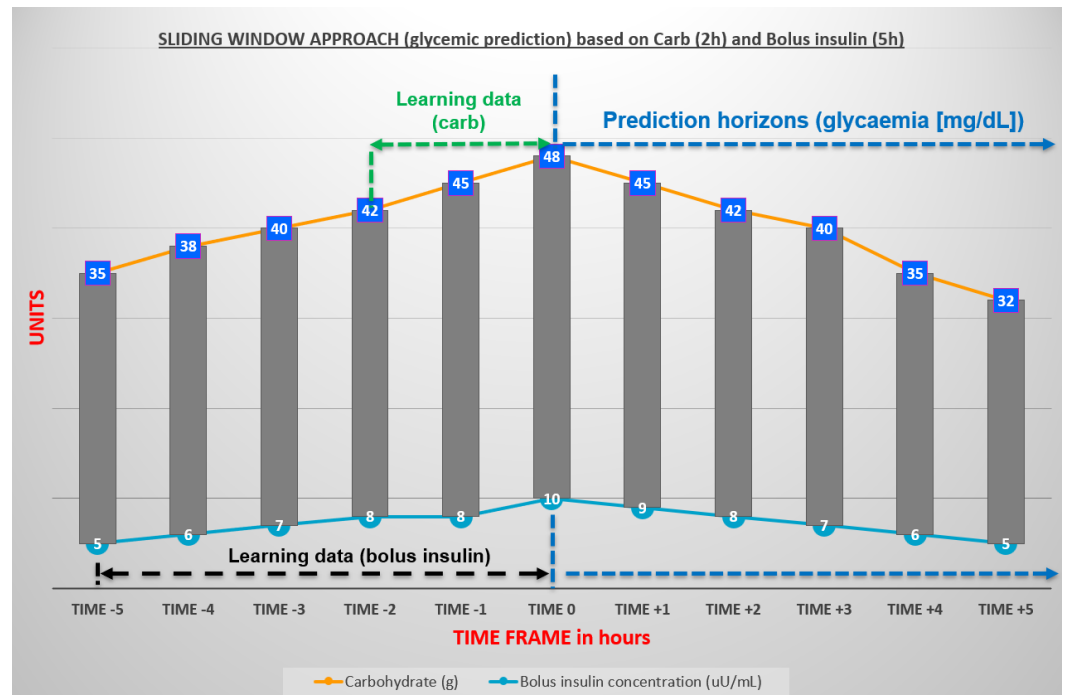


Figure 5. Sliding window approach for time series: carbohydrates and insulin.

represented by the green dashed left-right arrow to predict the oscillation glucose up to 8 hours (blue dashed line). 303
304

5. Results 305

Tesseractus was implemented as a Python [53] prototype. Its set up was conducted 306
considering data collected from seven T1D Brazilian volunteers, during a week. The 307
volunteers profiles are described at table 3, where it is given their id, sex, age, abdominal 308
circumference (AC), and body mass (BM). In addition, table 4 presents the time of collection 309
data, the origin of glucose values, and type of insulin with a concentration of 100 units per 310
mL (100U/mL). Other data collected from the T1D individual were the HbA1c (hemoglobin 311
A1c) value and whether they were hypertensive (1) or not (0), in order to calculate the eGDR 312
(mg/(kg.minute)) of each individual (table 5). The ID is only to identify the individual. 313

Table 3. Characteristics of each individual.

ID	Sex (M/F)	Age (years)	AC (cm)	BM (kg)
R-BRA01	F	36	79	57
R-BRA02	M	50	115	90
R-BRA03	M	28	91	70
R-BRA04	M	45	132	120
R-BRA05	M	39	93	83
R-BRA06	M	39	91	78
R-BRA07	F	65	90	68

An example of how it is possible to analyze the behavior of each individual is repre- 314
sented in figure 6, for volunteer R-BRA07. His profile is characterized in tables 3, 4 and 315
5: R-BRA07 is non-hypertensive, his hemoglobin A1c is 7.5%, yielding an eGDR of 9.34 316
(mg/kg.minute). The glucose rate of ascent and descent was collected every 30 minutes, 317
between midnight and 8am, during 14 days. These data were compared with the Tesseractus 318
prediction ones and further plotted in a Parkes Error Grid [54] (sec. 5.1). It is possible to 319

Table 4. Satellite characteristics to collect data.

ID	Days	Source	Insulin
R-BRA01	14	FreeStyle Libre [®]	aspart + degludec
R-BRA02	21	Minimed 640G [®]	lispro
R-BRA03	14	FreeStyle Libre [®]	aspart + degludec
R-BRA04	21	Minimed 640G [®]	lispro
R-BRA05	14	FreeStyle Libre [®]	aspart + glargine
R-BRA06	21	Paradigm VEO 754 [®]	lispro
R-BRA07	14	FreeStyle Libre [®]	lispro + degludec

Table 5. Information to calculate estimated glucose disposal rate (eGDR).

ID	Hypertensive	HbA1c (%)	eGDR
R-BRA01	0	5	11.7
R-BRA02	1	6	4.51
R-BRA03	0	6.3	9.91
R-BRA04	1	5.6	3.2
R-BRA05	0	8	8.8
R-BRA06	0	6	10
R-BRA07	0	7.5	9.34

notice that there is a tendency for the glucose concentration to fall in the early hours of the morning, but for example, there is a rise every day from five in the morning. The glucose oscillation is quite peculiar and can be affected by the dawn phenomenon, which is characterized by hyperglycemia during morning early morning [55]. Another factor that influences the continuity of the glucose concentration increase is having breakfast almost every day at six o'clock with carbohydrate intake.

5.1. Testing and Validation

Through the natural competition established between the Math and ML agents, with their respective strategies, it was possible to establish the best result between them and practice a continuous flow of active Reinforcement Learning, using historical data from seven volunteers for up to 21 days. The best result is always closer to the ideal glucose range: 80-120 mg/dL in fasting and up to 160 mg/dL in the postprandial period.

Daytime and nighttime windows were personalized for each individual (6), with the addition of information related to their usual sleeping hours (nighttime) and active hours (daytime). Such personalization is needed to decide whether Tesseractus must be fed by new external stimulus. This is needed because our prediction horizon for nighttime is 8 hours, at most, and individuals with nighttime windows greater than that must have their prediction horizon updated.

Table 6. Volunteers' nighttime and daytime windows.

ID	nighttime	daytime
R-BRA01	10:41pm – 07:59am	08:00am – 10:40pm
R-BRA02	10:01pm – 05:59am	06:00am – 10:00pm
R-BRA03	10:01pm – 07:59am	08:00am – 10:00pm
R-BRA04	09:16pm – 08:59am	09:00am – 09:15pm
R-BRA05	11:59pm – 07:34am	07:35am – 11:58pm
R-BRA06	09:51pm – 05:29am	05:30am – 09:50pm
R-BRA07	08:51pm – 05:59am	06:00am – 08:50pm

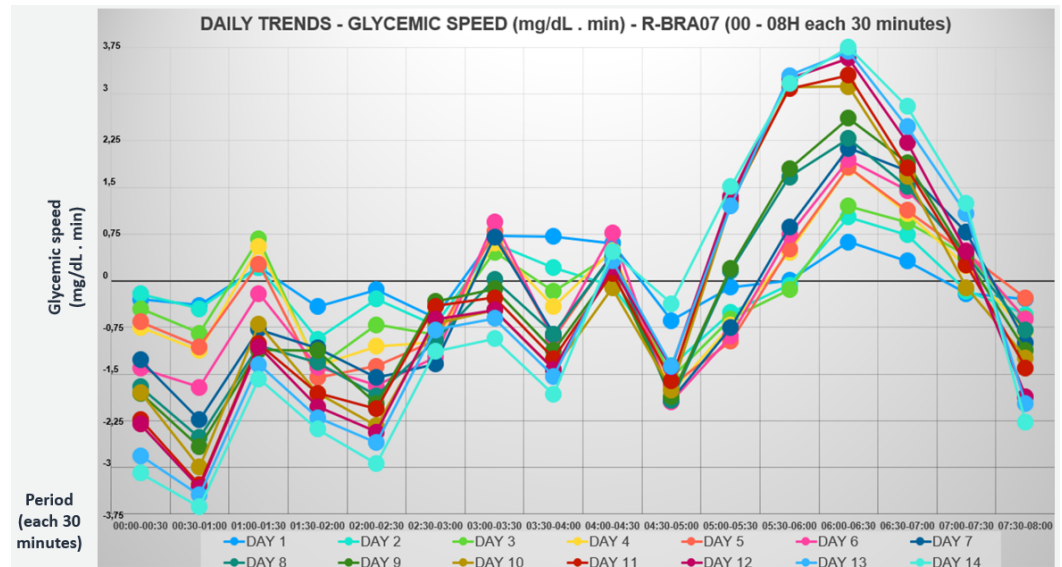


Figure 6. Ascent and descent glucose rate from individual R-BRA07: nighttime.

We use the Parkes Error Grid (PEG) [56] to evaluate errors in the measurement of predicted glucose oscillation provided by Tesseract. It was adopted because it is compliant with ISO15197 [57] and it separates TD1 individuals from individuals with type 2 DM. Moreover, PEG had its technical issues revised by Pfitzner and colleagues (2013), who established exact borders for the performance zones for glucose measurements and support the accuracy definition for glucose monitors. The zones are categorized as **A**, **B**, **C**, **D** and **E**. The associate meaning for a measurement of being in a zone is: **zone A** – clinically accurate measurements, no effect on clinical action; **zone B** – altered clinical action, little or no effect on clinical outcome; **zone C** – altered clinical action, likely to affect clinical outcome; **zone D** – altered clinical action, could have significant clinical risk; **zone E** – altered clinical action, could have dangerous consequences.

PEG was used considering the predicted **versus** measured values, and the success metric is simple: the most prediction points that fall within zones A and B, the better is the model. Table 7 details the PEG for the daytime window considering each prediction horizon (PH) (from 15 minutes to 4 hours). It can be depicted that 95.1% of measurements, on average, fall on zones A and B. The same result is presented in Figure 7, showing a total of 3,126 predictions. Zones A and B are the closest ones to the diagonal line of the plot.

Table 7. Results of Parkes Error Grid for Tesseract (zones) - daytime period.

PH	A (%)	B (%)	C (%)	D (%)	E (%)	A+B (%)
Average	62.3	32.8	4.4	0.5	0	95.1
15 min	93	6.8	0.2	0	0	99.8
30 min	76.9	22.2	0.8	0	0	99.1
60-min	56.4	41.5	2	0.1	0	97.9
90 min	50.1	44.9	4.7	0.3	0	95
120 min	50.3	41.8	7.4	0.5	0	92.1
180 min	46	44	8.9	0.9	0.2	90
240 min	49.6	40.4	9.7	0.3	0	90

For the nighttime window, table 8 details the PEG of each PH (from 15 minutes to 8 hours). It can be depicted that 93.7% of measurements, on average, fall on zones A and B. The same result is presented in Figure 8, showing a total of 1,400 predictions. It is important to observe that for a PH of 480 min (8 hours), the Tesseract model presented PEG of 95% falling between zones A and B.

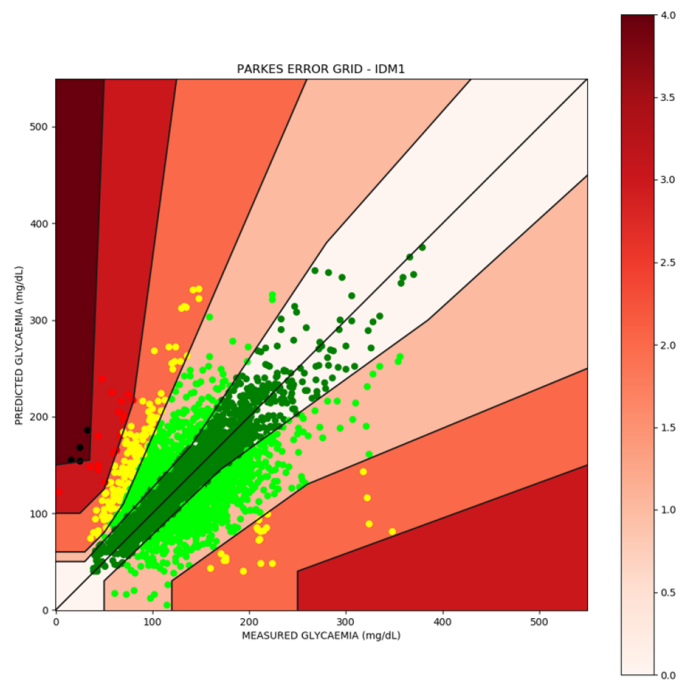


Figure 7. Parkes Error Grid (daytime period) for seven T1D individuals. Green dots lay at zones A and B (95.1% on average): 3,804 predictions.

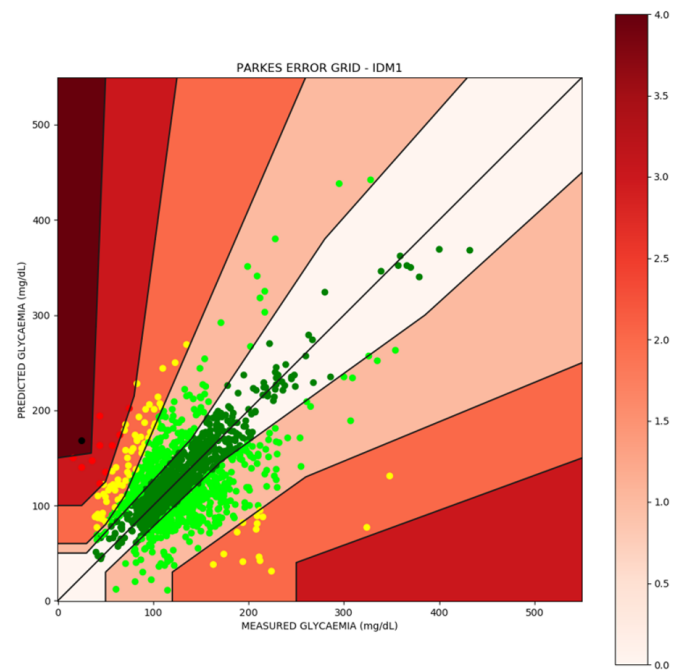


Figure 8. Parkes Error Grid (night period) for seven T1D individuals. Green dots lay at zones A and B (93.7% on average): 1,400 predictions.

Table 8. Results of Parkes Error Grid for Tesseractus (zones) - night period.

PH	A (%)	B (%)	C (%)	D (%)	E (%)	A+B (%)
Average	55.8	37.9	5.6	0.7	0	93.7
15 min	86	12.4	1.7	0	0	98.4
30 min	72.2	26.9	0.9	0	0	99.1
60 min	57.1	41.8	1.1	0	0	98.9
90 min	50	44.4	5.6	0	0	94.4
120 min	47.7	46.7	5.6	0	0	94.4
180 min	45.3	44.7	8.6	0.7	0.6	90
240 min	48.8	42.2	8.4	0.6	0	91
300 min	46.2	44.8	8	1.2	0	91
360 min	54.2	37.8	6.5	1.5	0	92
420 min	52.3	39.7	6.7	1.3	0	92
480 min	62	33	4.5	0.5	0	95

Among other well-known error evaluation metrics such as MAPE (mean absolute percentage error), MAE (mean absolute error) and, RMSE (root mean square error), we consider MAE and MAPE the most relevant to evaluate the success of our model, because T1D individuals need predictions as closer as the real measurements as possible. Thus, the lower the MAE and MAPE values, the better the model is in relation to the prediction.

Table 9. MAE - daytime and nighttime comparison concerning seven T1D individuals.

PH	Daytime (avg - mg/dL)	Nighttime (avg - mg/dL)
Tesseractus	24.56	27.77
15 min	9.18	9.27
30 min	16.97	16.09
60 min	26.41	26.26
90 min	30.24	28.09
120 min	30.54	28.3
180 min	33.61	32.68
240 min	25.01	34.49
300 min	–	35.16
360 min	–	34.97
420 min	–	33.96
480 min	–	26.37

In fact, such metrics is calculated considering absolute values for the difference (measured value minus predicted glucose concentration). Therefore, we evaluate MAE and MAPE considering such error for all PHs, and organized them for daytime and nighttime in the tables 9 and 10, respectively. It is important to note that daytime window run from 15 to 240 minutes and nighttime window from 15 to 480 min.

6. Discussion

Both results linked to PEG analysis and MAE are pioneers, due to the long-term prediction horizons, e.g. 7 or 8 hours for nighttime. At the best of our knowledge, there is not literature presenting these prediction horizons. However, we compared Tesseractus with other models that address shorter PH. In fact, whenever we consider PEG, we can cite [37] and [58], for a PH of one hour. In one hand, in [37] Munoz-Organero considered nine real individuals and obtained a PEG of 87.22% falling in zones A+B, while in [58] Foss-Freitas *et al.* considered 21 real individuals and obtained a Clarke Error Grid (CEG) of 94% falling in zones A+B. It is worth noting that both PEG and CEG are comparable error grids [59].

Table 10. MAPE - daytime and nighttime comparison concerning seven T1D individuals.

PH	Daytime (%)	Nighttime (%)
Tesseractus	22.01	25.51
15 min	8	7.84
30 min	13.32	14.43
60 min	20.52	22.78
90 min	24.98	28.11
120 min	30.79	28.04
180 min	33.26	31.19
240 min	37.82	30.57
300 min	–	23.96
360 min	–	36.49
420 min	–	32
480 min	–	25.33

Tesseractus outperformed both for the same PH, achieving a PEG of 97.9% falling in zones A+B for daytime and 98.9% at nighttime.

Whenever we consider MAE as the error, we can cite [60], who obtained MAE equal to 51.3 mg/dL for PH of 60 minutes while Tesseractus reached 26.41 mg/dL, both in daytime. It is worth noting that the smaller the MAE, the better the values. Finally, if the considered error is MAPE, Foss-Freitas *et al.* (2019) presented interesting results for PH ranging from 30 to 360 minutes. A comparison with Tesseractus is presented in table 11 considering nighttime PH. Observe that Tesseractus outperform them for PH of 120, 180 and 360 minutes, being 360 min the highest PH they achieve. Nevertheless, they outperform Tesseractus for short PH like 30 and 60 minutes. We advocate that this is not an issue, since the need for long-term prediction is paramount for nighttime.

Table 11. MAPE at nighttime - mean comparison between Foss-Freitas *et al.* (2019) and Tesseractus - 21 days of training

PH	Foss-Freitas <i>et al.</i> (2019) (%)	Tesseractus (%)
30 min	7	14.43
60 min	16.8	22.78
120 min	32.7	28.04
180 min	45	31.19
360 min	44.2	36.49
420 min	–	32
480 min	–	25.33

In addition to the results achieved, it is worth mentioning the main contributions of the Tesseractus model, in a summarized way: (1) Combination of different techniques in the same model working in an orchestrated way, from mathematics to ML (supervised and reinforcement learning), represented by agents; (2) Continuous learning for applicability in real individuals with T1D; (3) Using a MAS, it was possible to delegate the task of continuous self-adjustment process about prediction errors (4) Tesseractus works independently of sex and age; (5) It was tested with 7 real individuals; (6) Applicability in technology-based healthcare; (7) Prediction of glycemic oscillation of up to 8 hours, depending on the individual's lifestyle, with acceptable absolute error; (8) support for personalized recommendations about on macronutrients, insulin and physical exercise, based on ML models, not just fixed rules.

This indicates the feasibility of Tesseractus to be applied as the underlying model to: an open artificial pancreas [62]; an artificial pancreas (closed-loop) [48]; insulin pumps [63],[64]; and a recommendation system, to cite a few. It is our claim that it must facilitate

daily life of T1D individuals, automating most of the individual T1D's 180 extra daily health-related decisions [65].

7. Conclusions

The paper presented Tesseractus, a hybrid model that adopts a multi-agent approach to address the problem of predicting glucose concentration for T1D individuals. Tesseractus has reactive and intelligent agents, where the reactive agents act as sensors and monitors, and intelligent agents act as an oracle or as an apprentice. The oracle knowledge is provided by a mathematical model for the HGIRS and it transfer knowledge to the apprentice, which also learn from data provided by sensors and monitors. Tesseractus uses a dual continuous learning model, which can mitigate errors between the predicted and continuously measured values, in addition to the ODE's, that describes the HGIRS, own input parameters. The combination of techniques is advantageous, as it consists of models with complementary functions, resulting in a cohesive, well-adjusted model capable of generalization.

Tesseractus was validated with seven real T1D Brazilian individuals, that provided their data collected up to 21 days: the seven initial days were used to personalize the model and the following days were used to validate the model capacity of predicting glucose oscillation for PH that range from 15min to 4 hours during daytime and from 15min to 8 hours at night period. As the evaluation of the Mean Absolute Error (MAE) indicates, Tesseractus is able to predict glucose oscillation with an accuracy equal to or less than 30 mg/dL (1.7 mmol/L). As future work, it is our intention to continuously improve the performance of the Tesseractus while reducing the error of the predicted value, by removing some specific restrictions found in the literature: (a) constant values of parameters from mathematical models for prediction calculations; (b) agent's support for continuous learning and ODE parameter values correction; (c) barriers to combine different prediction models, using Active Learning, reusing, combining and adapting knowledge from different agents [51].

Some limitations need to be addressed in future work such as: (1) It does not support pregnant women and type 2 individuals com diabetes mellitus; (2) For now it only supports 4 types of insulin analogues: aspart, lispro, glargine and degludec; (3) The dataset is still small, performed with historical data for only seven real individuals; (4) Few insulin sensors or pumps were tested during the research, according to the table 4; (5) It is necessary test with new variables: stress, hormonal effects, blood oxygen, heart rate; (6) Analyze blood glucose and insulin concentration associated with comorbidities.

Author Contributions: For research articles with several authors, a short paragraph specifying their individual contributions must be provided. The following statements should be used: Conceptualization, J.P., A.A., J.S and M.L.; methodology, J.P. and A.A.; software, J.P.; validation, J.P., A.A. and J.S.; formal analysis, J.P. and J.S; investigation, J.P.; resources, J.A. and A.A; data curation, J.P.; writing—original draft preparation, J.P.; writing—review and editing, J.P., A.A., J.S and M.L.; visualization, J.P.; supervision, J.P. and A.A; project administration, J.P. and A.A.. All authors have read and agreed to the published version of the manuscript.

Funding: This research received no external funding

Institutional Review Board Statement: The study was conducted in accordance with the Declaration of Helsinki, and approved by the Ethics Committee of the University Hospital of São Paulo (HU-USP) (protocol code 1819188 - approved on 09/24/2021), for studies involving humans.

Informed Consent Statement: Informed consent was obtained from all subjects involved in the study (Free and Informed Consent Term).

Data Availability Statement: Not applicable.

Conflicts of Interest: The authors declare no conflict of interest.

Abbreviations

The following abbreviations are used in this manuscript:

AC	Abdominal Circumference
AP	Artificial Pancreas
BG	Blood Glucose
BM	Body Mass
CGM	Continuous Glucose monitoring
CNS	Central Nervous System
DM	Diabetes Mellitus
EGA	Error Grid Analysis
eGDR	estimated Glucose Disposal Rate
HBA1C	Glycated hemoglobin
HGIRS	Humamn Glucose-Insulin Regulatory System
HGP	Hepatic Glucose Production
IDF	International Diabetes Federation
IT1D	Individuals with T1D
MAE	Mean Absolute Error
MAS	Multi-agent System
ML	Machine Learning
ODE	Ordinary Differential Equations
PEG	Parkes Error Grid
RMSE	Root Mean Square Error
PH	Prediction Horizon
SBD	Brazilian Society of Diabetes
T1D	Type 1 Diabetes Mellitus
TEX	Time of Exercise
VO2	Volume of Oxygen

References

1. SBD. *Diretrizes da Sociedade Brasileira de Diabetes - Guidelines of the Brazilian Society of Diabetes*, 2022. <https://diretriz.diabetes.org.br> [Accessed: 2022-01-10].
2. Magliano, D.; et al.. *IDF Diabetes Atlas: Global, regional and country-level diabetes prevalence estimates for 2021 and projections for 2045*. *Diabetes Research and Clinical Practice* **2022**, 183. <https://diabetesatlas.org> [Accessed: 2022-03-15].
3. Kissler, S.; Cichowitz, C.; S. Sankaranarayanan, S.; Bortz, D. *Determination of personalized diabetes treatment plans using a two-delay model*. *Journal of Theoretical Biology* **2014**, 359, 101–111. <https://doi.org/10.1016/j.jtbi.2014.06.005> [Accessed: 2019-08-08].
4. Russell, S.J.; Norvig, P. *Artificial Intelligence: A Modern Approach*, 3 ed.; Pearson Education, 2016.
5. Ramírez, A.; Pérez-Aguila, R. *A Method for Obtaining the Tesseract by Unraveling the 4D Hypercube*. In Proceedings of the The 10-th International Conference in Central Europe on Computer Graphics, Visualization and Computer Vision'2002, WSCG 2002, University of West Bohemia, Campus Bory, Plzen-Bory, Czech Republic, February 4-8, 2002, pp. 1–8. http://wscg.zcu.cz/wscg2002/Papers_2002/E37.pdf [Accessed: 2020-07-06].
6. Shlomo, M.; Auchus, R.; Goldfine, A.; Koenig, R.; Rosen, C. *Williams Textbook of Endocrinology*, 14 ed.; Elsevier, 2019.
7. Gardner, D.; Shoback, D. *Greenspan's Basic & Clinical Endocrinology*, 10 ed.; Mc Graw Hill, 2018.
8. Georga, E.I.; Protopappas, V.C.; Ardigò, D.; Marina, M.; Zavaroni, I.; Polyzos, D.; Fotiadis, D.I. *Multivariate prediction of subcutaneous glucose concentration in type 1 diabetes patients based on support vector regression*. *IEEE journal of biomedical and health informatics* **2013**, 17, 71–81. <https://pubmed.ncbi.nlm.nih.gov/23008265/> [Accessed: 2017-10-05].
9. Liu, C.; Vehí, J.; Avari, P.; Reddy, M.; Oliver, N.; Georgiou, P.; Herrero, P. *Long-Term Glucose Forecasting Using a Physiological Model and Deconvolution of the Continuous Glucose Monitoring Signal*. *Sensors (Basel)* **2019**, 19, 4338. <https://doi.10.3390/s19194338> [Accessed: 2021-07-29].
10. Cescon, M.; Johansson, R.; Renard, E. *Subspace-based linear multi-step predictors in type 1 diabetes mellitus*. *Biomedical Signal Processing and Control* **2015**, 22, 99–110. <https://www.sciencedirect.com/science/article/pii/S1746809414001475> [Accessed: 2022-01-10].
11. Vu, L.; Kefayati, S.; Idé, T.; Pavuluri, V.; Jackson, G.; Latts, L.; Zhong, Y.; Agrawal, P.; Chang, Y. *Predicting Nocturnal Hypoglycemia from Continuous Glucose Monitoring Data with Extended Prediction Horizon*. *AMIA Annu Symp Proc* **2020**, pp. 874–882. <https://pubmed.ncbi.nlm.nih.gov/32308884/> [Accessed: 2021-12-11].
12. Smith, H. *An Introduction to Delay Differential Equations with Applications to the Life Sciences*, 1 ed.; Texts in Applied Mathematics 57, Springer-Verlag New York, 2011.
13. Schindelboeck, D.; Praus, F.; Gall, W. *A Diabetes Self-Management Prototype in an AAL-Environment to Detect Remarkable Health States* **2016**. 223, 273–280. <https://pubmed.ncbi.nlm.nih.gov/27139414/> [Accessed: 2022-06-30].

14. Epstein, E.J.; Osman, J.L.; Cohen, H.W.; Rajpathak, S.N.; Lewis, O.; Crandall, J.P. *Use of the Estimated Glucose Disposal Rate as a Measure of Insulin Resistance in an Urban Multiethnic Population With Type 1 Diabetes*. *Diabetes Care* **2013**, *36*, 2280–2285. <https://care.diabetesjournals.org/content/36/8/2280> [Accessed: 2018-05-28].
15. Nelson, R.K.; Horowitz, J.F.; Holleman, R.G.; Swartz, A.M.; Strath, S.J.; Kriska, A.M.; Richardson, C.R. *Daily physical activity predicts degree of insulin resistance: a cross-sectional observational study using the 2003–2004 National Health and Nutrition Examination Survey*. *International Journal of Behavioral Nutrition and Physical Activity* **2013**, *10*(1). <https://ijbnpa.biomedcentral.com/articles/10.1186/1479-5868-10-10> [Accessed: 2019-02-25].
16. Liu, C.; Vehi, J.; Oliver, N.; Georgiou, P.; Herrero, P. *Enhancing blood glucose prediction with meal absorption and physical exercise information* **2018**. <https://arxiv.org/abs/1901.07467> [Accessed: 2022-04-19].
17. SBD-EXERCISE., 2022. <https://diabetes.org.br/atividade-fisica/> [Accessed: 2022-05-16].
18. Bratusch-Marrain, P.; Komjati, M.; Waldhäusl, W. *Efficacy of pulsatile versus continuous insulin administration on hepatic glucose production and glucose utilization in type I diabetic humans*. *Diabetes* **1986**, *35*, 922–926. <https://pubmed.ncbi.nlm.nih.gov/3525288/> [Accessed: 2016-11-11].
19. Li, J.; Kuang, Y.; Mason, C. *Modeling the glucose–insulin regulatory system and ultradian insulin secretory oscillations with two explicit time delays*. *Journal of Theoretical Biology* **2006**, *242*, 722–735. <https://doi.org/10.1016/j.jtbi.2006.04.002> [Accessed: 2016-12-28].
20. Sturis, J.; Polonsky, K.; Mosekilde, E.; Cauter, E. *Computer model for mechanisms underlying ultradian oscillations of insulin and glucose*. *Am. J. Physiol.* **1991**, *260*, 1–10. <https://pubmed.ncbi.nlm.nih.gov/2035636/> [Accessed: 2021-03-05].
21. Tolić, I.M.; Mosekilde, E.; Sturis, J. *Modeling the insulin–glucose feedback system: the significance of pulsatile insulin secretion*. *Journal of theoretical biology* **2000**, *207*, 361–375. https://ui.adsabs.harvard.edu/link_gateway/2000JThBi.207..361T/doi:10.1006/jtbi.2000.2180 [Accessed: 2016-08-01].
22. FDA-Glargine., 2022. https://www.accessdata.fda.gov/drugsatfda_docs/label/2007/021081s024lbl.pdf [Accessed: 2021-09-10].
23. FDA-Degludec., 2022. https://www.accessdata.fda.gov/drugsatfda_docs/label/2015/203314lbl.pdf [Accessed: 2021-09-10].
24. FDA-Lispro., 2022. https://www.accessdata.fda.gov/drugsatfda_docs/label/2003/20563scm044_humalog_lbl.pdf [Accessed: 2018-05-28].
25. FDA-Aspart., 2022. https://www.accessdata.fda.gov/drugsatfda_docs/label/2012/020986s057lbl.pdf [Accessed: 2021-09-10].
26. Owens, D.R.; Bailey, T.S.; Fanelli, C.; Yale, J.F.; Bolli, G. *Clinical relevance of pharmacokinetic and pharmacodynamic profiles of insulin degludec (100, 200 U/mL) and insulin glargine (100, 300 U/mL)—a review of evidence and clinical interpretation*. *Diabetes & Metabolism* **2019**, *45*, 330–340. <https://doi.org/10.1016/j.diabet.2018.11.004> [Accessed: 2020-11-10].
27. Porcellati, F.; Rossetti, P.; Ricci, N.B.; Pampanelli, S.; Torlone, E.; Campos, S.H.; Andreoli, A.M.; Bolli, G.B.; Fanelli, C.G. *Pharmacokinetics and pharmacodynamics of the long-acting insulin analog glargine after 1 week of use compared with its first administration in subjects with type 1 diabetes*. *Diabetes care* **2007**, *30*, 1261–1263. <https://diabetesjournals.org/care/article/30/5/1261/29895/Pharmacokinetics-and-Pharmacodynamics-of-the-Long> [Accessed: 2022-08-10].
28. Abe, S.; Inoue, G.; Yamada, S.; Irie, J.; Nojima, H.; Tsuyusaki, K.; Usui, K.; Atsuda, K.; Yamanouchi, T. *Two-way crossover comparison of insulin glargine and insulin detemir in basal-bolus therapy using continuous glucose monitoring*. *Diabetes, Metabolic Syndrome and Obesity: Targets and Therapy* **2011**, *4*, 283. <https://pubmed.ncbi.nlm.nih.gov/21792327/> [Accessed: 2019-05-16].
29. Barnett, A.H. *Insulin glargine in the treatment of type 1 and type 2 diabetes*. *Vascular health and risk management* **2006**, *2*, 59. <https://doi.org/10.2147/vhrm.2006.2.1.59> [Accessed: 2020-01-30].
30. Linnebjerg, H.; Lam, E.C.Q.; Seger, M.E.; Coutant, D.; Chua, L.; Chong, C.L.; Ferreira, M.M.; Soon, D.; Zhang, X. *Comparison of the pharmacokinetics and pharmacodynamics of LY2963016 insulin glargine and EU-and US-approved versions of Lantus insulin glargine in healthy subjects: three randomized euglycemic clamp studies*. *Diabetes Care* **2015**, *38*, 2226–2233. <https://doi.org/10.2337/dc14-2623> [Accessed: 2020-07-15].
31. SANOFI-Lantus., 2020. <http://products.sanofi.ca/en/lantus.pdf> [Accessed: 2020-12-12].
32. Slattery, D.; Amiel, S.; Choudhary, P. *Optimal prandial timing of bolus insulin in diabetes management: a review*. *Diabetic Medicine* **2018**, *35*, 306–316. <https://doi.org/10.1111/dme.13525> [Accessed: 2022-08-17].
33. Plank, J.; Wutte, A.; Brunner, G.; Siebenhofer, A.; Semlitsch, B.; Sommer, R.; Hirschberger, S.; Pieber, T.R. *emphA direct comparison of insulin aspart and insulin lispro in patients with type 1 diabetes*. *Diabetes care* **2002**, *25*, 2053–2057. <http://dx.doi.org/10.2337/diacare.25.11.2053> [Accessed: 2021-3-29].
34. de la Peña, A.; Seger, M.; Soon, D.; Scott, A.J.; Reddy, S.R.; Dobbins, M.A.; Brown-Augsburger, P.; Linnebjerg, H. *Bioequivalence and comparative pharmacodynamics of insulin lispro 200 U/mL relative to insulin lispro (Humalog®) 100 U/mL*. *Clinical Pharmacology in Drug Development* **2016**, *5*, 69–75. <https://doi.org/10.1002/cpdd.221> [Accessed: 2021-07-15].
35. FDA-Lispro(a), 2022. https://www.accessdata.fda.gov/drugsatfda_docs/label/2007/020563s082lbl.pdf [Accessed: 2022-01-27].
36. Contreras, I.; Bertachi, A.; Biagi, L.; Vehí, J.; Oviedo, S. *Using Grammatical Evolution to Generate Short-term Blood Glucose Prediction Models*. In Proceedings of the KHD@ IJCAI, 2018, pp. 91–96. <http://ceur-ws.org/Vol-2148/paper15.pdf> [Accessed: 2019-11-01].
37. Munoz-Organero, M. *Deep Physiological Model for Blood Glucose Prediction in T1DM Patients*. *Sensors* **2020**, p. 3896. <https://doi.org/10.3390/s20143896> [Accessed: 2021-08-16].
38. Zarkogianni, K.; Litsa, E.; Vazeou, A.; Nikita, K.S. *Personalized glucose–insulin metabolism model based on self-organizing maps for patients with Type 1 Diabetes Mellitus*. In Proceedings of the 13th IEEE International Conference on BioInformatics and BioEngineering. IEEE, 2013, pp. 1–4. <https://doi.org/10.1109/BIBE.2013.6701604> [Accessed: 2016-12-28].

39. Saiti, K.; Macaš, M.; Lhotská, L.; Štechová, K.; Pithová, P. *Ensemble methods in combination with compartment models for blood glucose level prediction in type 1 diabetes mellitus*. *Computer Methods and Programs in Biomedicine* **2020**, *196*, 105628. <https://doi.org/10.1016/j.cmpb.2020.105628> [Accessed: 2022-02-25]. 543-545
40. Bunesco, R.; Struble, N.; Marling, C.; Shubrook, J.; Schwartz, F. *Blood glucose level prediction using physiological models and support vector regression*. In Proceedings of the 2013 12th International Conference on Machine Learning and Applications. IEEE, 2013, Vol. 1, pp. 135–140. <https://doi.org/10.1109/ICMLA.2013.30> [Accessed: 2018-06-09]. 546-548
41. Bertachi, A.; Biagi, L.; Contreras, I.; Luo, N.; Vehí, J. *Prediction of Blood Glucose Levels And Nocturnal Hypoglycemia Using Physiological Models and Artificial Neural Networks*. In Proceedings of the KHD@ IJCAI, 2018, pp. 85–90. <http://ceur-ws.org/Vol-2148/paper14.pdf> [Accessed: 2020-12-08]. 549-551
42. Mirshekarian, S.; Bunesco, R.; Marling, C.; Schwartz, F. *Using LSTMs to learn physiological models of blood glucose behavior*. In Proceedings of the 2017 39th Annual International Conference of the IEEE Engineering in Medicine and Biology Society (EMBC). IEEE, 2017, pp. 2887–2891. <https://doi.org/10.1109/embc.2017.8037460> [Accessed: 2019-08-13]. 552-554
43. Wang, W.; Wang, S.; Wang, X.; Liu, D.; Geng, Y.; Wu, T. *A Glucose-Insulin Mixture Model and Application to Short-Term Hypoglycemia Prediction in the Night Time*. *IEEE Transactions on Biomedical Engineering* **2020**. <https://ieeexplore.ieee.org/document/9163275> [Accessed: 2021-04-06]. 555-557
44. Isfahani, M.K.; Zekri, M.; Marateb, H.R.; Faghihimani, E. *A hybrid dynamic wavelet-based modeling method for blood glucose concentration prediction in type 1 diabetes*. *Journal of Medical Signals and Sensors* **2020**, *10*, 174–184. https://doi.org/10.4103/jmss.jmss_62_19 [Accessed: 2021-10-05]. 558-560
45. Zecchin, C.; Facchinetti, A.; Sparacino, G.; Cobelli, C. *Jump neural network for online short-time prediction of blood glucose from continuous monitoring sensors and meal information*. *Computer methods and programs in biomedicine* **2014**, *113*, 144–152. <https://doi.org/10.1016/j.cmpb.2013.09.016> [Accessed: 2016-12-18]. 561-563
46. Hajizadeh, I.; Rashid, M.; Turksoy, K.; Samadi, S.; Feng, J.; Sevil, M.; Hobbs, N.; Lazaro, C.; Maloney, Z.; Littlejohn, E.; et al. *Incorporating unannounced meals and exercise in adaptive learning of personalized models for multivariable artificial pancreas systems*. *Journal of diabetes science and technology* **2018**, *12*, 953–966. <https://pubmed.ncbi.nlm.nih.gov/30060699/> [Accessed: 2020-08-30]. 564-566
47. Amigoni, F.; Dini, M.; Gatti, N.; Somalvico, M. *Anthropic agency: a multiagent system for physiological processes*. *Artificial Intelligence in Medicine* **2003**, *27*, 305–334. <https://www.sciencedirect.com/science/article/pii/S0933365703000083> [Accessed: 2017-11-18]. 567-568
48. FDA-ControllIQ., 2022. <https://www.fda.gov/news-events/press-announcements/fda-authorizes-first-interoperable-automated-insulin-dosing-controller-designed-allow-more-choices> [Accessed: 2022-06-30]. 569-570
49. Brown, S.A.; Kovatchev, B.P.; Raghinaru, D.; Lum, J.W.; Buckingham, B.A.; Kudva, Y.C.; Laffel, L.M.; Levy, C.J.; Pinsky, J.E.; Wadwa, R.P.; et al. *Six-Month Randomized, Multicenter Trial of Closed-Loop Control in Type 1 Diabetes*. *New England Journal of Medicine* **2019**, *381*, 1707–1717. <https://doi.org/10.1056/NEJMoa1907863> [Accessed: 2021-04-02]. 571-573
50. Rodríguez, I.R. *Gestión de la Diabetes Mellitus Tipo 1 con Dispositivos Internet de las Cosas y Técnicas de Aprendizaje Automático*. PhD thesis, Universidad de Murcia, 2020. <http://hdl.handle.net/10201/87361> [Accessed: 2021-09-18]. 574-575
51. Kholghi, M.; Sitbon, L.; Zuccon, G.; Nguyen, A. *Active learning: a step towards automating medical concept extraction*. *Journal of the American Medical Informatics Association* **2015**, *23*, 289–296. <https://doi.org/10.1093/jamia/ocv069> [Accessed: 2018-12-01]. 576-577
52. Alfian, G.; Syafrudin, M.; Rhee, J.; Anshari, M.; Mustakim, M.; Fahrurrozi, I. *Blood Glucose Prediction Model for Type 1 Diabetes based on Extreme Gradient Boosting*. *IOP Conference Series: Materials Science and Engineering* **2020**, *803*, 012012. <https://doi.org/10.1088/1757-899x/803/1/012012> [Accessed: 2022-01-30]. 578-580
53. PYTHON., 2022. <https://www.python.org/> [Accessed: 2018-11-01]. 581
54. Pfützner, A.; Klonoff, D.; Pardo, S.; Parkes, J. *Technical aspects of the Parkes Error Grid*. *Journal of diabetes science and technology* **2013**, *7*, 1275–1281. <https://doi.org/10.1177/193229681300700517> [Accessed: 2017-05-08]. 582-583
55. Furutani, E. *Closed-loop blood glucose control for type 1 diabetes*, journal = Electronics and Communications in Japan **2019**. *102*, 22–26. <https://onlinelibrary.wiley.com/doi/abs/10.1002/ecj.12179> [Accessed: 2020-09-02]. 584-585
56. Parkes, J.L.; Slatin, S.L.; Pardo, S.; Ginsberg, B.H. *A new consensus error grid to evaluate the clinical significance of inaccuracies in the measurement of blood glucose*. *Diabetes Care* **2000**, *23*, 1143–1148. <https://doi.org/10.2337/diacare.23.8.1143> [Accessed: 2018-07-15]. 586-587
57. Pleus, S.; Baumstark, A.; Jendrike, N.; Mende, J.; Link, M.; Zschornack, E.; Haug, C.; Freckmann, G. *System accuracy evaluation of 18 CE-marked current-generation blood glucose monitoring systems based on EN ISO 15197:2015*. *BMJ Open Diabetes Research and Care* **2020**, *8*. <https://drc.bmj.com/content/8/1/e001067.full.pdf> [Accessed: 2021-11-18]. 588-590
58. Foss-Freitas, M.C.; Moreira, G.S.; Antloga, V.P.; Neto, C.R.; Rodrigues, E.M.; Matsumoto, Y.K. *Accuracy Analysis of an Autonomous System to Personalize Blood Glucose Prediction for T1DM Patients with Real World Data*. 2020. <https://doi.org/10.2337/db19-930-P> [Accessed: 2022-04-15]. 591-593
59. Klonoff, D.; Lias, C.; Vigersky, R.; Clarke, W.; Parkes, J.; Sacks, D.; Kirkman, M.; Kovatchev, B. *Error Grid Panel. The surveillance error grid*. *J Diabetes Sci Technol* **2014**, *8*, 658–72. 594-595
60. Zecchin, C.; Facchinetti, A.; Sparacino, G.; Cobelli, C. *How Much Is Short-Term Glucose Prediction in Type 1 Diabetes Improved by Adding Insulin Delivery and Meal Content Information to CGM Data? A Proof-of-Concept Study*. *Journal of Diabetes Science and Technology* **2016**, *10*, 1149–1160. <https://doi.org/10.1177/1932296816654161> [Accessed: 2018-10-01]. 596-598
61. Foss-Freitas, M.C.; Moreira, G.S.; Antloga, V.P.; Neto, C.R.; Rodrigues, E.M.; Da Costa, M.F.; Pereira, A.; Matsumoto, Y.K. *930-P: Blood Glucose Levels Prediction Accuracy for T1DM Patients Using Neural Networks to Combine Insulin Doses, Food Nutrients, and Heart Rate*. *Diabetes* **2019**, *68*. <https://doi.org/10.2337/db19-930-P> [Accessed: 2022-01-28], <https://doi.org/10.2337/db19-930-P>. 599-600

-
62. OpenAPS., 2022. <https://openaps.org/> [Accessed: 2022-07-02]. 602
63. MINIMED-640G., 2020. <https://www.medtronicdiabeteslatino.com/br/wp-content/uploads/2018/12/Sistema-Minimed-640G.pdf> [Accessed: 2021-03-21]. 603
64. CONTROL-IQ., 2020. 604
65. Tack, C.; Lancee, G.; Heeren, B.; Engelen, L.; Hendriks, S.; Zimmerman, L.; De Massari, D.; van Gelder, M.; van de Belt, T. *Glucose Control, Disease Burden, and Educational Gaps in People With Type 1 Diabetes: Exploratory Study of an Integrated Mobile Diabetes App. JMIR Diabetes* **2018**, *23*. <https://doi.org/10.2196/diabetes.9531> [Accessed: 2019-09-01]. 605
606
607
608